International Conference on Mathematics, Computational Methods & Reactor Physics (M&C 2009)
Saratoga Springs, New York, May 3-7, 2009, on CD-ROM, American Nuclear Society, LaGrange Park, IL (2009)

AUTOMATICALLY TUNED ADAPTIVE DIFFERENCING ALGORITHM FOR 3-D S_N IMPLEMENTED IN PENTRAN

Glenn Sjoden[1], Tanguy Courau[2,*], Kevin Manalo[1], and Ce Yi[1]
sjoden@ufl.edu, tanguy.courau@edf.fr, kmanalo@gmail.com, yice@ufl.edu
[1]University of Florida, Dept of Nuclear & Radiological Engineering, Gainesville, Florida, USA
[2]EDF R&D/SINETICS, 1 av du Général de Gaulle, F92141 Clamart CEDEX, France

ABSTRACT

We present an adaptive algorithm with an automated tuning feature to augment optimum differencing scheme selection for 3-D S_N computations in Cartesian geometry. This adaptive differencing scheme has been implemented in the PENTRAN parallel S_N code. Individual fixed zeroth spatial transport moment based schemes, including Diamond Zero (DZ), Directional Theta Weighted (DTW), and Exponential Directional Iterative (EDI) 3-D S_N methods were evaluated and compared with solutions generated using a code-tuned adaptive algorithm. Model problems considered include a fixed source slab problem (using reflected *y*- and *z*-axes) which contained mixed shielding and diffusive regions, and a 17x17 PWR assembly eigenvalue test problem; these problems were benchmarked against multigroup MCNP5 Monte Carlo computations. Both problems were effective in highlighting the performance of the adaptive scheme compared to single schemes, and demonstrated that the adaptive tuning handles exceptions to the standard DZ-DTW-EDI adaptive strategy. The tuning feature includes special scheme selection provisions for optically thin cells, and incorporates the ratio of the angular source density relative to the total angular collision density to best select the differencing method. Overall, the adaptive scheme demonstrated the best overall solution accuracy in the test problems.

KEYWORDS: 3-D S_N, Adaptive Differencing, Automatic Tuning, Parallel

1. INTRODUCTION

Many Sn differencing schemes have been formulated over the years since the introduction of the discrete ordinates (S_N) method by Carlson [1]. One of the challenges of solving diverse deterministic transport problems is that the differencing scheme employed must perform well in diffusive as well as streaming regions, both of which can occur in the same local spatial mesh in the case of neutron transport as neutrons down-scatter. This paper presents an *adaptive differencing* algorithm with *automatic tuning* for 3-D discrete ordinates applications. While this concept has been introduced before [4, 5, 6, 7], the tuning feature enables the adaptive algorithm to correctly apply the most accurate scheme as changes occur in problem physics. The updated adaptive scheme described here, incorporating the new EDI scheme, was implemented into the PENTRAN parallel discrete ordinates S_N solver in Cartesian Coordinates. The spatial mesh distribution in PENTRAN uses a block coarse mesh/fine mesh discretization, enabling different mesh densities to be specified in localized zones, established according to the needs of the engineer in representing radiation transport problem geometry. Adaptive mesh refinement, where the spatial mesh is refined to adjust to problem physics, is costly for solvers decomposed on parallel computers; alternatively, PENTRAN adjusts the S_N differencing algorithm on a stable spatial coarse mesh/fine mesh grid. Initially, in any one coarse mesh zone, the adaptive algorithm begins with the traditional diamond difference scheme with a zero negative fixup algorithm,

[*]Currently appointed as visiting research scientist at the University of Florida

hereafter referred to as Diamond Zero (DZ). If fixups are recorded, the Directional Theta Weighted (DTW) algorithm is selected; then, if gradients become too steep using DTW, the recently introduced Exponential Directional Iterative (EDI) scheme [8] is used. Moreover, mechanisms are in place in the adaptive logic sequence so that the optimal application of a differencing scheme is implemented over the phase space of the problem. In this paper, we briefly present each scheme in the adaptive sequence, and discuss the details of the adaptive algorithm, including the new tuning logic to indicate how each scheme is selected. Following this, we present a classic model shielding test problem and an eigenvalue problem used in our evaluation of differencing schemes, comparing our solutions with multigroup Monte Carlo reference solutions. This is followed by a brief discussion and conclusions.

2. OVERVIEW OF ADAPTIVE SCHEMES

The steady state, Legendre expanded multigroup form of the transport equation in 3-D Cartesian geometry is [2]:

$$(\mu\frac{\partial}{\partial x}+\eta\frac{\partial}{\partial y}+\xi\frac{\partial}{\partial z})\psi_g(x,y,z,\mu,\varphi)+\sigma_g(x,y,z)\psi_g(x,y,z,\mu,\varphi)=$$

$$\sum_{g'=1}^{G}\sum_{l=0}^{L}(2l+1)\sigma_{s,g'\to g,l}(x,y,z)\{P_l(\mu)\phi_{g',l}(x,y,z)+2\sum_{k=1}^{l}\frac{(l-k)!}{(l+k)!}P_l^k(\mu)\cdot$$

$$[\phi^k_{C\,g',l}(x,y,z)\cos(k\varphi)+\phi^k_{S\,g',l}(x,y,z)\sin(k\varphi)]\}+\frac{\chi_g}{k_o}\sum_{g'=1}^{G}\nu\sigma_{f\,g'}(x,y,z)\phi_{g',0}(x,y,z) \qquad (1a)$$

where

$\mu,\eta,\xi =$ x, y, z direction cosines, respectively, for angular ordinate

$\psi_g =$ group g angular particle flux (for groups $g=1,G$)

$\varphi =$ azimuthal angle constructed from $\arctan(\xi/\eta)$, with proper phase shift

$\sigma_g =$ total group macroscopic cross section

$l =$ Legendre expansion index ($l = 0, L$), L=0 or odd truncation

$\sigma_{sg'\to g,l} = l$ th Legendre moment of the macroscopic differential scattering cross section from group $g' \to g$

$P_l(\mu) = l$ th Legendre polynomial

$\phi_{g',l} = l$ th Legendre scalar flux moment for group g

$P_l^k(\mu) = l$ th , k th Associated Legendre polynomial

$\phi^k_{C\,g',l} = l$ th , k th Cosine Associated Legendre scalar flux moment for group g

$\phi^k_{S\,g',l} = l$ th , k th Sine Associated Legendre scalar flux moment for group g

$\chi_g =$ group fission distribution constant (neutrons)

$k_o =$ criticality eigenvalue (neutrons)

$\nu\sigma_{f\,g} =$ group fission production (neutrons)

The flux moments, $\phi_{g',l}$, $\phi^k_{C\,g',l}$ and $\phi^k_{S\,g',l}$ are defined in terms of μ' and φ' as:

$$\phi_{g',l}(x,y,z) = \int_{-1}^{1} \frac{d\mu'}{2} P_l(\mu') \int_0^{2\pi} \frac{d\varphi'}{2\pi} \psi_{g'}(x,y,z,\mu',\varphi') \tag{1b}$$

$$\phi^k_{C\,g',l}(x,y,z) = \int_{-1}^{1} \frac{d\mu'}{2} P^k_l(\mu') \int_0^{2\pi} \frac{d\varphi'}{2\pi} \cos(k\varphi') \psi_{g'}(x,y,z,\mu',\varphi') \tag{1c}$$

$$\phi^k_{S\,g',l}(x,y,z) = \int_{-1}^{1} \frac{d\mu'}{2} P^k_l(\mu') \int_0^{2\pi} \frac{d\varphi'}{2\pi} \sin(k\varphi') \psi_{g'}(x,y,z,\mu',\varphi') \tag{1d}$$

Allowing for only *m* discrete directions, a spatial approximation to Equation (1) is required by considering a cell volume has parallelepiped dimensions $(\Delta x, \Delta y, \Delta z)$, and assuming edge and center flux integrals are represented by surface and volumetric averages, the zeroth moment balance equation in 3-D Cartesian coordinates is (omitting group subscripts for brevity):

$$\frac{|\mu_m|}{\Delta x}(\psi_{\text{out}\,x} - \psi_{\text{in}\,x}) + \frac{|\eta_m|}{\Delta y}(\psi_{\text{out}\,y} - \psi_{\text{in}\,y}) + \frac{|\xi_m|}{\Delta z}(\psi_{\text{out}\,z} - \psi_{\text{in}\,z}) + \sigma\psi_A = q_A \tag{2}$$

Equation (2) contains surface averaged terms enter and leave the cell along each axis using "in" and "out" subscripts, respectively, dependent upon the propogation of radiation through the cell along a direction $\hat{\Omega}_m$, and "*A*" subscripts denote cell average quantities. Equation (2) is exact, but contains seven unknowns. Three entrant values ("in" surface averages) are known from boundary values or as exiting fluxes from surrounding cells, and that the collective cell averaged volumetric source q_A is assumed to be known from a previous source iteration (in the standard Sn source iteration scheme). As a result, only the cell averaged angular flux ψ_A and the exiting ("out") surface values are unknowns; these values are derived based on a set of auxiliary equations. For weighted spatial differencing schemes, the following auxiliary equations are assumed to hold between cell average and boundary angular fluxes:

$$\begin{aligned}
\psi_{\text{out}\,x} &= \frac{1}{a}(\psi_A + \psi_{\text{in}\,x}(a-1)) \\
\psi_{\text{out}\,y} &= \frac{1}{b}(\psi_A + \psi_{\text{in}\,y}(b-1)) \\
\psi_{\text{out}\,z} &= \frac{1}{c}(\psi_A + \psi_{\text{in}\,z}(c-1))
\end{aligned} \tag{3}$$

The Diamond Differencing (DD) scheme results when a=½, b=½, and c=½ in Equations (3); DD is second order accurate, but may lead to negative solutions [2]. In such situations, a "negative flux set to zero fixup" of the Diamond scheme is commonly used, denoted as Diamond Zero (DZ). In addition to being non-physical, the negative flux fixup can also cause load imbalance during parallel processing. Petrovic and Haghighat developed the Directional Theta-Weighted (DTW) scheme [3] that is a modification of Rhoades and Engle's strictly positive Theta Weighted scheme.

For the DTW scheme, to force positivity for the x-axis term, the lower bound of $\psi_{\text{out } x}$ is strictly zero, and we obtain an equation for the "*a*" weight in Equation (3):

$$a = 1 - \frac{q_A + \frac{|\mu_m|}{\Delta x}\psi_{\text{in } x} + \theta(\mu_m)\left(\frac{|\eta_m|}{\Delta y}\psi_{\text{in } y} + \frac{|\xi_m|}{\Delta z}\psi_{\text{in } z}\right)}{\left(2\frac{|\eta_m|}{\Delta y} + 2\frac{|\xi_m|}{\Delta z} + \sigma\right)\psi_{\text{in } x}} \tag{4}$$

A similar procedure is applied along the *y*- and *z*-axes to yield weights for "*b*" and "*c*" in Equation (3). The cell averaged angular flux for the DTW scheme is given by [6, 9]:

$$\psi_A = \frac{q_A + \frac{|\mu_m|}{a\Delta x}\psi_{\text{in } x} + \frac{|\eta_m|}{b\Delta y}\psi_{\text{in } y} + \frac{|\xi_m|}{c\Delta z}\psi_{\text{in } z}}{\left(\frac{|\mu_m|}{a\Delta x} + \frac{|\eta_m|}{b\Delta y} + \frac{|\xi_m|}{c\Delta z} + \sigma\right)} \tag{5}$$

The auxiliary equation for the Exponential Directional Iterative (EDI) scheme is formed initially from an exponential auxiliary equation [8]:

$$\psi_m(x,y,z) = a_o \; exp(\lambda_i \, P_1(x)/|\,\mu_m|\,) \; exp(\lambda_j \, P_1(y)/|\,\eta_m|\,) \; exp(\lambda_k \, P_1(z)/|\,\xi_m|\,) \tag{6}$$

where $P_1(u) = (2u/\Delta u - 1)$ are first order spatial Legendre functions (orthogonal to 0^{th} order equations with unit weight) over the widths of a single cell. EDI is a predictor-corrector scheme where angular fluxes from the DTW scheme are used to start a fixed point iteration to refine each exponential constant $\lambda_i, \lambda_j, \lambda_k$ by *successive iteration (I-1, I, I+1…)* of Equations (7):

$$\lambda_{i,I} = f(\lambda_{i,I-1}) = \frac{(\psi_{out\,x}(\lambda_{i,I-1}) - \psi_{in\,x}(\lambda_{i,I-1}))\,|\,\mu_m\,|}{2\psi_A(\lambda_{i,I-1})}$$

$$\lambda_{j,I} = g(\lambda_{j,I-1}) = \frac{(\psi_{out\,y}(\lambda_{j,I-1}) - \psi_{in\,y}(\lambda_{j,I-1}))\,|\,\eta_m\,|}{2\psi_A(\lambda_{j,I-1})}$$

$$\lambda_{k,I} = h(\lambda_{k,I-1}) = \frac{(\psi_{out\,z}(\lambda_{k,I-1}) - \psi_{in\,z}(\lambda_{k,I-1}))\,|\,\xi_m\,|}{2\psi_A(\lambda_{k,I-1})} \tag{7}$$

These exponential constants are converged through successive iteration, typically two; the fixed point iteration will remain convergent on a finite, nonzero interval [*p*,*q*] by adhering to the first derivative criterion in Equations (8):

$$\left|\frac{\partial f\,(\lambda_{i,I-1})}{\partial \lambda_{i,I-1}}\right| < 1 \qquad \left|\frac{\partial g\,(\lambda_{j,I-1})}{\partial \lambda_{j,I-1}}\right| < 1 \qquad \left|\frac{\partial h\,(\lambda_{k,I-1})}{\partial \lambda_{k,I-1}}\right| < 1 \tag{8}$$

The EDI volume averaged angular flux is given in Equations (9a) and (9b):

$$\psi_A = \left(\exp(\frac{2\lambda_i}{|\mu_m|})-1\right)\left(\exp(\frac{2\lambda_j}{|\eta_m|})-1\right)\left(\exp(\frac{2\lambda_k}{|\xi_m|})-1\right)\frac{1}{\beta}\left(q_A+\frac{|\mu_m|}{\Delta x}\psi_{in\,x}+\frac{|\eta_m|}{\Delta y}\psi_{in\,y}+\frac{|\xi_m|}{\Delta z}\psi_{in\,z}\right) \tag{9a}$$

With the β term given as:

$$\begin{aligned}\beta = {} & \frac{2\lambda_i}{\Delta x}\left(\exp(\frac{2\lambda_i}{|\mu_m|})\right)\left(\exp(\frac{2\lambda_j}{|\eta_m|})-1\right)\left(\exp(\frac{2\lambda_k}{|\xi_m|})-1\right)+ \\ & \frac{2\lambda_j}{\Delta y}\left(\exp(\frac{2\lambda_j}{|\eta_m|})\right)\left(\exp(\frac{2\lambda_i}{|\mu_m|})-1\right)\left(\exp(\frac{2\lambda_k}{|\xi_m|})-1\right)+ \\ & \frac{2\lambda_k}{\Delta z}\left(\exp(\frac{2\lambda_k}{|\xi_m|})\right)\left(\exp(\frac{2\lambda_i}{|\mu_m|})-1\right)\left(\exp(\frac{2\lambda_j}{|\eta_m|})-1\right)+ \\ & \sigma\left(\exp(\frac{2\lambda_i}{|\mu_m|})-1\right)\left(\exp(\frac{2\lambda_j}{|\eta_m|})-1\right)\left(\exp(\frac{2\lambda_k}{|\xi_m|})-1\right)\end{aligned} \tag{9b}$$

Outbound fluxes can be defined in terms of the average angular flux:

$$\begin{aligned}\psi_{\text{out }x} &= \psi_A\frac{2\lambda_i}{|\mu_m|}\left(1-\exp(\frac{-2\lambda_i}{|\mu_m|})\right)^{-1} \\ \psi_{\text{out }y} &= \psi_A\frac{2\lambda_j}{|\eta_m|}\left(1-\exp(\frac{-2\lambda_j}{|\eta_m|})\right)^{-1} \\ \psi_{\text{out }z} &= \psi_A\frac{2\lambda_k}{|\xi_m|}\left(1-\exp(\frac{-2\lambda_k}{|\xi_m|})\right)^{-1}\end{aligned} \tag{10}$$

Therefore, the EDI scheme is implemented using an initial starting guess from DTW, with successive applications of Equations (7), (9), and (10) applied in accordance with Equations (8) to yield a stable fixed-point iteration to solve for more accurate values of each exponential constant $\lambda_i, \lambda_j, \lambda_k$. The *adaptive differencing* strategy in PENTRAN, determined individually for each coarse mesh zone, works in the following manner: assume (for illustration) that the DZ scheme is initially assigned in each coarse mesh region containing a number of fine meshes. An automatic differencing scheme upgrade from DZ to DTW takes place if a negative flux fixup is encountered anywhere in the coarse mesh. This is potentially followed later by another transfer from DTW to EDI if any maximum DTW linear weight factor (*a*,*b*,*c*) exceeding a user specified maximum weight factor is detected for DTW within a coarse mesh. This is performed since a high weight factor indicates DTW is being pressed to maintain positivity (at the expense of accuracy) in a severe streaming environment, so that the shift to EDI enables an exponential treatment for cells that are optically thick, since these scenarios are best handled using the exponentially based auxiliary function of the EDI scheme.

A novel "Tuning Feature" handles exceptions to the standard adaptive strategy for the Adaptive differencing strategy, and this feature calls for special provisions for optically thin cells, as well as evaluation of the angular source density relative to the total angular collision density in a parameter called the "*qfratio*". First, consider that $\Delta h_{\max} = \max(\Delta x, \Delta y, \Delta z)$ is computed to evaluate the optical cell thickness $\sigma \Delta h_{\max}$; for a given coarse mesh, if this optical thickness is less than a user specified value (e.g. 0.02, used as the default in PENTRAN), then for these "vanishingly thin" cells, the DTW scheme is *not* upgraded to the EDI scheme for any circumstance, since a very small optical thickness is such that DTW is perfectly adequate to accurately resolve the angular flux, and an exponential treatment is not needed.

Moreover, as mentioned, upgrades from DTW to EDI are based on any DTW weight factor (*a,b,c*) exceeding a value approaching unity (e.g. a default of 0.95 in PENTRAN), where in a streaming situation with no or low-level sources, weight factors near unity are required to maintain positivity at the expense of accuracy. However, high weight factors can also occur in any mesh cell that contains a strong source, simply because the angular flux in these situations is shallow or relatively *flat* (resulting in low angular flux gradients)—this is the opposite of the streaming case. Therefore, with a strong source present, this leads to DTW weight factors close to unity, and causes a conflict with the standard upgrade criteria; this is undesirable, since the DTW scheme performs very well in regions where there is a strong source—DTW weight factors are close to unity because the flux is inherently flat. Therefore, if the angular flux is inherently flat due to the presence of a strong source, a step scheme would be very effective—the "step" scheme results algebraically if the weights are set to unity along each direction for DTW. This scenario has been mitigated for the adaptive differencing methodology in *PENTRAN* through the use of the *qfratio* parameter.

Considering the group dependent transport equation divided through by the collision density term, with group sources denoted using scatter, fission, and independent source variables:

$$\frac{\hat{\Omega} \cdot \nabla \psi_g}{\sigma_g \psi_g} + 1 = \frac{(q_{sg} + q_{fg} + q_{ind\,g})}{\sigma_g \psi_g} = qfratio \qquad (11)$$

The *qfratio* is the computed ratio of the cell total angular source density to the cell angular collision density; a *qfratio* > 1.00 indicates a "source dominated" cell, and a *qfratio* < 1.00 indicates a "streaming dominated" cell, where "source" includes the combined scatter, fission, and independent angular source terms. Note this simple relationship is readily available when solving for angular fluxes within each cell. If the *qfratio* is greater than a user prescribed value (the default for *qfratio* = 1.00 in PENTRAN), then the DTW scheme is automatically selected without regard to the DTW weight factors, since in a source dominated cell, the DTW scheme performs optimally, and exponential treatment with EDI is not applicable. Therefore, with the *qfratio* parameter, upgrades will *only* occur when the fine mesh cell is one that is "streaming dominated" away from source regions.

3. NUMERICAL TESTING

To test the adaptive scheme, we employed two model problems. Model Problem 1 is Slab geometry fixed source differencing scheme test problem originally used in a paper by Alcouffe, et al [10], which contains a mix of both streaming and diffusive regions. This is an excellent problem for evaluating the performance of our adaptive scheme with tuning. Model Problem 2 is a criticality eigenvalue problem for a typical PWR 17x17 assembly model with complete reflection and with fuel cells (pins and surrounding moderator) individually (locally) homogenized with a lattice pitch of 1.26 cm.

3.1. Slab Model Problem: Detailed Description

A schematic of the slab fixed source Model Problem 1 depicting the four coarse meshes is given in Figure 1. This problem is subdivided into 4 coarse meshes, with each coarse mesh zone numbered sequentially from left to right; the first zone is a half-scattering region; the second zone has a source and is a pure absorber; the third zone contains a typical shield; the fourth zone is a diffusive region. Unit density sources are placed in the second (absorbing) and fourth (diffusive) coarse mesh regions; the problem is set up to use reflective boundaries for both *y*- (vertical) and *z*- axes (out of the page), with vacuum boundaries on either end (*x*-axis). The four coarse mesh boundaries span the *x*-axis from [0, 3.0, 6.0, 36.0, 48.0] cm.

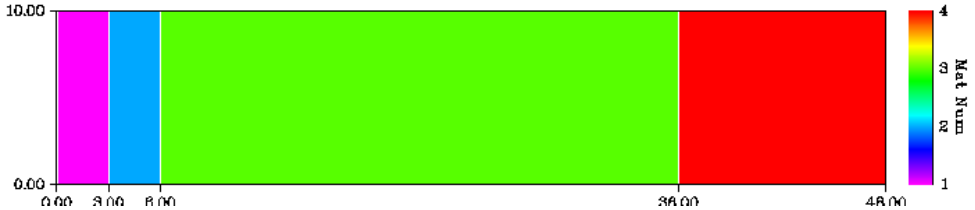

Figure 1. Fixed Source Slab "Model Problem 1" Coarse Mesh Cells, Numbered 1 to 4, left to right

Cross sections for this problem in each respective zone are given in Table 1. Again, material 1 is a 3.0 cm thick half-scattering material; material 2 is a 3.0 cm thick pure absorber with a source; material 3 is 30.0 cm thick shield material; material 4 is a 12.0 cm diffusive region with a source.

Table 1. Slab Model Problem One-Group Cross Sections (P_0), Source Terms (units in 1/cm)

HalfScat	Material 1		
Sigma_a	nuSigma_f	Sigma_t	Sigma_s
0.5	0.00	1.00	0.5000
Src+PureAbs	Material 2	Source =1 n/cc/s	
Sigma_a	nuSigma_f	Sigma_t	Sigma_s
1.0	0.00	1.00	1E-6
Shield	Material 3		
Sigma_a	nuSigma_f	Sigma_t	Sigma_s
0.95	0.00	1.00	0.0500
Src+Diff	Material 4	Source =1 n/cc/s	
Sigma_a	nuSigma_f	Sigma_t	Sigma_s
0.05	0.00	1.00	0.9500

To be consistent with the problem posed, a *reference mesh* in each region (the number of meshes in the *x*-direction) was specified (60, 60,600,240) for each coarse mesh, with the DZ algorithm,

respectively. The quadrature specified for this problem was S_8, with an inner convergence tolerance of 1E-05. In addition, two single group MCNP5 models were executed, the first with no adjoint weighting, and the second with adjoint weighted weight windows, to yield an independent solution metric for comparison.

In comparison to the aforementioned *reference mesh* case in PENTRAN, the mean volumetric cell fluxes by material region, normalized to the # of source MCNP particles, were calculated for materials 1 through 4. Table 2 offers the percent error for two cases run in MCNP. The first case is a multigroup MCNP5 run mode using the MGOPT (multigroup) option (without adjoint weighting). The second case employs adjoint weighted weight windows using the WWINP option in multigroup mode (MGOPT). The adjoint weighted weight windows were generated with PENTRAN using the *reference mesh* in adjoint mode, with automated WWINP generation performed with an auxilary code written in Fortran called PENIMP. Running with adjoint weighted weight windows offers the advantage of a higher figure or merit (FOM) and improved overall relative error for a fixed computer time (or even for a fixed number of histories, as shown for 1E08 histories). The maximum MCNP5 cell/material F4 flux tally error is also reported.

Table 2. Percent error by material/CM# (PENTRAN *reference mesh* S_N case is error basis)

Case (nps = 1E08 for each)	M1 % error	M2 % error	M3 % error	M4 % error	Max Cell Flux R.E.	F4 Tally M3 FOM
MCNP5 - Multigroup	-1.216%	0.311%	-0.407%	0.134%	0.001	147104
MCNP5 - Multigroup with WWINP adjoint	-1.258%	0.288%	-0.401%	0.138%	0.0023	211977

3.2. 1/30th Mesh Solution to Model Problem 1

The problem was solved on 1/30th of the reference mesh using fixed schemes DZ, DTW, and the Adaptive scheme. In these cases, as shown in Figure 2, the adaptive differencing scheme was the most accurate scheme.

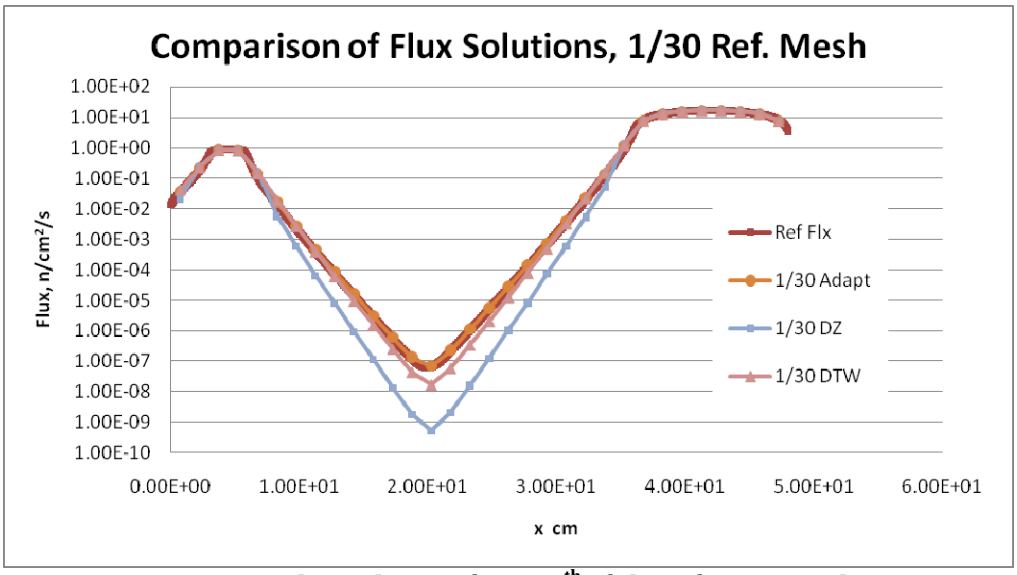

Figure 2. Flux Solutions for 1/30th of the reference mesh

3.3. 1/60th Mesh Solution to Model Problem 1

The Slab Model Problem was solved on 1/60th of the reference mesh using fixed schemes DZ, DTW, EDI, and the Adaptive scheme; this corresponds to a single fine mesh each in Coarse Mesh zones 1 and 2, with 10 fine mesh cells in Coarse Mesh 3, and 4 fine mesh cells in Coarse Mesh 4. The globally fixed DZ scheme did not converge at all with this low level of discretization, and had 100% error after hundreds of iterations. The DTW fixed scheme solution converged in 65 iterations, but over-predicted the flux by two orders of magnitude; the EDI-only rendered solution converged in 67 iterations, and upon observation was closest to the Adaptive solution. However, the Adaptive scheme solution was the most accurate, and converged in 66 iterations; for the adaptive scheme, Coarse Meshes 1 and 3 ended up using the EDI scheme, while Coarse Meshes 2 and 4 ended up remaining with the DZ scheme, as no fixups were needed. Again, the ideal nature of this concept is that the scheme applied is via code logic.

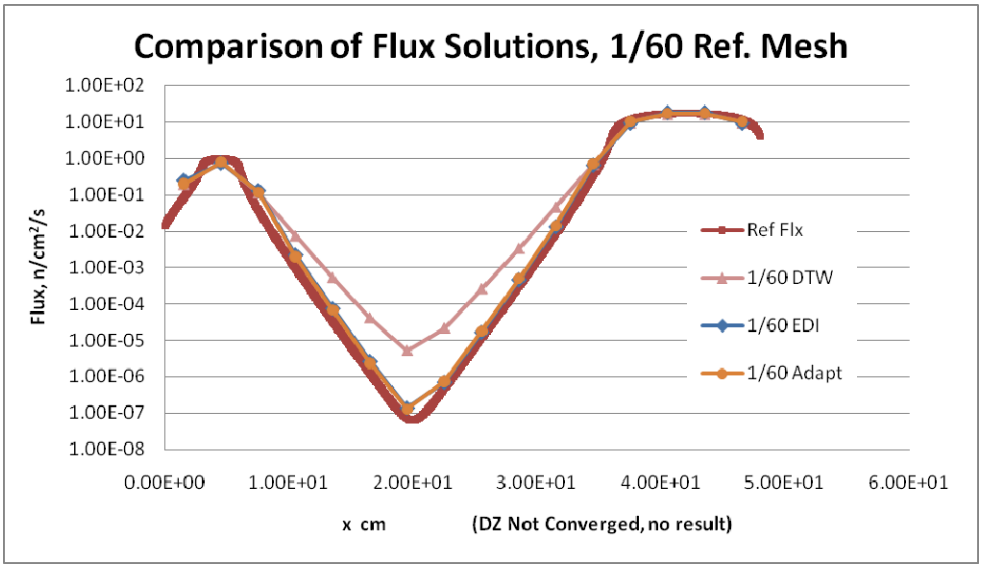

Figure 3. Flux Solutions for 1/60th of the reference mesh

To more effectively highlight the differences between the methods on the 1/60th mesh models, it is useful to compare errors in fluxes averaged over each of the Coarse Meshes, achieved by comparing with fluxes from the high resolution reference mesh solution. In doing so, a relative error computed according to

$$\varepsilon = \left| \frac{\phi_{TEST} - \phi_{REFERENCE}}{\phi_{REFERENCE}} \right| \tag{12}$$

was used to compare Coarse Mesh Average fluxes. In this comparsion, mean relative errors for the various differencing schemes were: Adaptive (11% error), DZ (100% error), DTW (13% error), and EDI (16% error). While the EDI scheme is highly effective in shielding problems due to an exponential based auxiliary formulation, this is not the best scheme to apply unilaterally when strong sources are present, since the natural updward concavity of the EDI scheme does not represent the flux well in source dominated regions.

3.4. Eigenvalue Model Problem: Detailed Description

A schematic of the criticality Model Problem 2 is given in Figure 4. This problem represents a PWR 17x17 assembly model with complete reflection and fuel cells (pins and surrounding moderator) individually homogenized with a lattice pitch of 1.26 cm; for modeling purposes the assembly was subdivided into 9 coarse mesh regions and two energy groups; each coarse mesh can independently employ a different differencing algorithm. Each fuel pin was associated with a material ID and a specific set of cross sections; accounting for symmetry, 45 materials were used. The total number of cells in each coarse mesh ranged from 1800 to 2592, totaling 20,808 fine mesh cells globally in the problem. From the previous example, it is clear that the adaptive scheme fared best, since the material properties and streaming effects were best handled with the adaptive strategy. The eigenvalue assembly problem posed a different challenge for the adaptive scheme, in that this problem has total reflection on all boundaries, so that gradients of the neutron flux were due to internal assembly pin-moderator-pin and neutron energy group coupled interactions, and the adaptive scheme is applicable only on a coarse mesh basis.

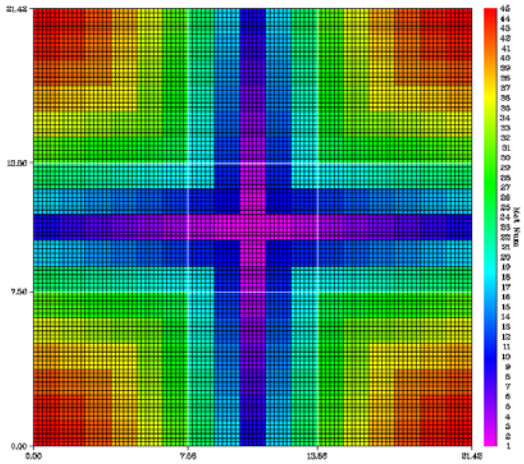

Figure 4. 17x17 PWR Assembly with 1.26 cm pin pitch; pin cells (fuel pin and moderator) are homogenized and subdivided into fine mesh cells contained in 9 coarse mesh cells

3.5. Differencing Scheme Comparisons for Model Problem 2

To determine the optimally performing differencing scheme, we compared solutions using two single differencing schemes (DZ and DTW) with the adaptive scheme for the eigenvalue problem. Since it is known that the assembly is a source dominated region, we did not attempt to implement a solution using the fixed EDI scheme unilaterally. Two refinements of quadrature were used for the testing, including S4 and S8, respectively, with the same spatial mesh. Comparison of the Group 1 and Group 2 fluxes from the adaptive cases using S8 quadrature with multigroup MCNP5 are included in Figure 5, and differ by no more than 0.4% in any one location.

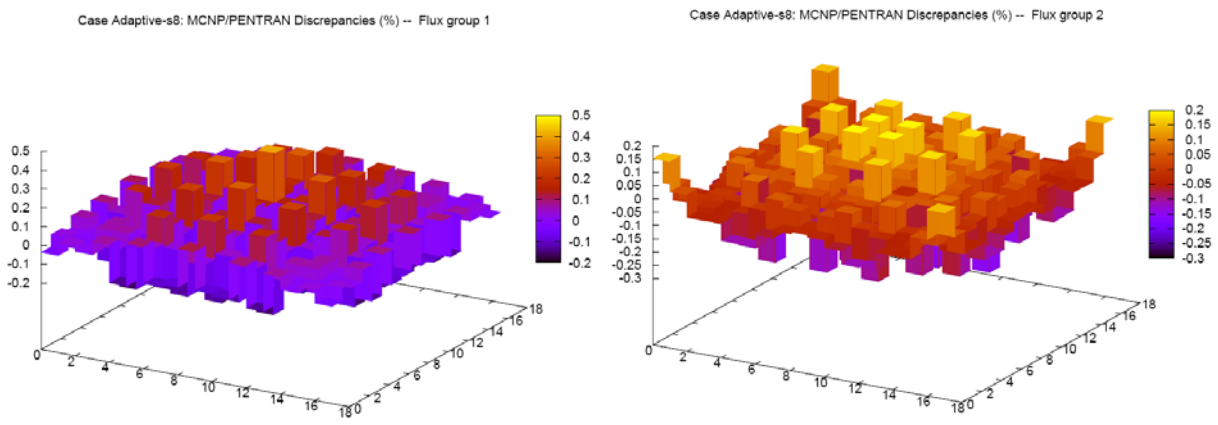

Figure 5. Comparison of group (G1, left; G2, right) flux percent differences between multigroup MCNP (P0) (σ<1%) and PENTRAN 'Adaptive S8' (ε=1E-5) solutions, 17x17 PWR Assembly

Multigroup MCNP5 results demonstrated that the k_{eff} of the assembly problem was 1.3714 (+/- 17 pcm). Comparing solutions, there were subtle differences in the results shown in Table 3.

Table 3. 17 x 17 Assembly Problem Results

Case:	Quadrature	Δk (pcm)	Δphi	(%)
Adaptive	s4	16	-0.56	0.64
DTW-locked	s4	16	-0.59	0.63
DZ-locked	s4	14	-0.46	0.61
Adaptive	s8	5	-0.28	0.4
DTW-locked	s8	11	-0.49	0.35
DZ-locked	s8	8	-0.24	0.4

As indicated, all S_4 and S_8 solutions fell within the uncertainty of the multigroup Monte Carlo solution; considering both the accuracy of Δk and flux (Δphi), the adaptive differencing scheme was the most accurate overall. Regarding timing, all schemes for the S_4 case required ~90 sec on 8 processors using both group and angular parallel decomposition. For the S_8 quadrature problems, the DZ and DTW fixed cases required ~260 sec, while the adaptive S_8 case required 560 sec, due to the fact that the optical thickness increased with the increased quadrature order, prompting selection of the EDI scheme in many parts of the problem, which is more expensive than DTW by nearly a factor of two. This is also an indicator that increasing quadrature order at this point would warrant mesh refinement.

4. CONCLUSIONS

In conclusion, we presented an adaptive algorithm with tuning for 3-D S_N computations in Cartesian geometry. Tests with the PENTRAN parallel S_N code using individual schemes versus the adaptive algorithm with tuning for a model slab problem and a 17x17 eigenvalue problem were conducted. The Model Problem (fixed source) contained mixed shielding and diffusive regions, and results clearly demonstrated that the adaptive scheme yielded the best overall solution accuracy. The eigenvalue problem demonstrated more consistency between the

schemes; however, the adaptive scheme still had the best overall accuracy, although the benefits of the adaptive scheme are less obvious on a problem with all reflective boundaries. In any case, it appears from these tests that the adaptive scheme with tuning, as described here, is quite effective when challenged with a problem with several zones differing in scattering properties.

REFERENCES

1. Carlson, B., "Solution of the Transport Theory Equation by the Sn Method," LA-1891, Los Alamos Scientific Laboratory (1955).

2. Lewis, E. E., and Miller, W.F., *Computational Methods of Neutron Transport,* American Nuclear Society, LaGrange Park, Illinois (1993).

3. Petrovic B., and Haghighat, A., "Analysis of Inherent Oscillations in Multidimensional Sn Solutions of the Neutron Transport Equation," *Nuclear Sci. and Eng.*, **124**, pp. 31-62 (1996).

4. Sjoden, G., and Haghighat, A., "A New Adaptive Differencing Strategy in the *PENTRAN* 3-D Parallel Sn Code", *Transactions of the American Nuclear Society*, **75** (1996).

5. Sjoden, G. E., and Haghighat, A., "PENTRAN - A 3-D Cartesian Parallel Sn Code with Angular, Energy, and Spatial Decomposition," *Proc of Joint Int'l Conf on Mathematical Methods and Supercomputing in Nuclear Apps.*, Saratoga, NY, Vol. II, p. 1267-1276 (1997).

6. Haghighat, A., and Sjoden, G., "Significance of Adaptive Differencing, Variable Grid Density, and TPMC for Sn Methods," *Proceedings of the 1999 Mathematics and Computation Conference on Reactor Physics and Supercomputing for Nuclear Applications*, Madrid, Spain, pp. 1775-1783 (1999).

7. Haghighat, A., Sjoden, G. E., and Kucukboyaci V., "Effectiveness of PENTRAN's Unique Numerics for Simulation of the Kobayashi Benchmarks", *Special Issue, Progress in Nuclear Energy Journal,* "3D Rad. Transport Benchmarks for Simple Geometries with Void Region," **39**, Nr. 2, ISSN 0149-1970 (2001).

8. Sjoden, G., "An Efficient Exponential Directional Iterative Differencing Scheme for 3-D Sn Computations in XYZ Geometry," *Nuclear Sci. and Eng*, Vol 155, pp. 179-189 (2007).

9. Sjoden, G. E., and Haghighat, A., *PENTRAN - Parallel Environment Neutral-particle TRANsport Version 9.4X.5,* Code Manual/Users Guide, HSW Technologies LLC, (2008).

10. Alcouffe, R.E., Larsen, E.W., Miller, W.F., Jr., and Wienke, B.R., "Computational Efficiency of Numerical Methods for the Multigroup Discrete Ordinates Neutron Transport Equations: The Slab Geometry Case, *Nuclear Sci. and Eng.*, Vol 71, pp.111-127 (1979).

11. X-5 MCNP5 Monte Carlo Development Team, "MCNP – A General Monte Carlo N-Particle Transport Code, Version 5, Volume II: MCNP User's Guide", LANL, Los Alamos, New Mexico, (2005), LA-CP-03-0245.